

TITLE: OPTICAL DIAGNOSTICS OF CO₂ LASER-FUSION TARGETS
USING BACKSCATTERED LIGHT

AUTHOR(S): D. E. Casperson, P-1

MASTER

SUBMITTED TO: Conference on Optics '81

University of California



DISCLAIMER
This book was prepared as an account of work sponsored by an agency of the United States Government. Neither the United States Government nor any agency thereof nor any of their employees makes any warranty, express or implied, or assumes any legal liability or responsibility for the accuracy, completeness, or usefulness of any information, apparatus, product, or process disclosed, or represents that its use would not infringe privately owned rights. Reference herein to any specific commercial product does not imply its endorsement, recommendation, or approval by the United States Government or any agency thereof. The views and opinions of authors expressed herein do not necessarily state or reflect those of the United States Government or any agency thereof.

By acceptance of this article, the publisher recognizes that the U.S. Government retains a nonexclusive, royalty-free license to publish or reproduce the published form of this contribution, or to allow others to do so, for U.S. Government purposes.

The Los Alamos Scientific Laboratory requests that the publisher identify this article as work performed under the auspices of the U.S. Department of Energy.

LOS ALAMOS SCIENTIFIC LABORATORY

Post Office Box 1663 Los Alamos, New Mexico 87545

An Affirmative Action/Equal Opportunity Employer

524

OPTICAL DIAGNOSTICS OF CO₂ LASER-FUSION TARGETS
USING BACKSCATTERED LIGHT*

D. E. Casperson
University of California
Los Alamos National Laboratory
Los Alamos, NM 87545

Abstract

With the f/2.4 focusing optics on one of the eight Helios CO₂ laser beam lines, direct backscattered light from a variety of glass microballoon targets has been observed. The quantities that have been measured include: (1) the total backscattered energy; (2) relative amplitudes of the backscattered fundamental and low harmonics ($n=1, 2, 3$) of the 10.6 μm incident light; (3) the 3/2 harmonic emission from a double pulse backscatter experiment; (4) the temporally resolved 10.6 μm light using a fast pyroelectric detector and a Los Alamos 5-GHz oscilloscope; and (5) the time-integrated spectrally resolved fundamental using a 3/4 meter spectrometer and a high resolution pyroelectric detector array (resolution $\sim 40 \text{ \AA}$ at 10.6 μm). The suitability of these diagnostics for evaluating the CO₂ laser plasma in terms of stimulated scattering processes, plasma density gradients, velocity of the critical surface, etc., is discussed.

*Work performed under the auspices of the U. S. Dept. of Energy.

Introduction

Although most of the primary diagnostics of laser-driven pellets in the inertial confinement fusion (ICF) program are close-in diagnostics, being on the order of 0.1-1 m distant from the targets and observing such quantities as x-rays, fast ions and neutrons, there is a class of useful diagnostics which can be utilized quite distant from the targets. These optical diagnostics sample target scattered laser light which contains useful information about the laser-matter interaction in the pellet. Depending upon optical layout of the system, the scattered light can be routed away from the target interaction area and hence away from the severe EMI and x-ray environment associated with these high-power short-pulse lasers. This scattered light can be spectrally, temporally, and spatially resolved to provide some understanding of the absorption process at the target plasma "critical" surface. This is the surface where the density of electrons is such that the local plasma frequency $\omega_p = (4\pi ne^2/m)^{1/2}$ is equal to the laser frequency ω_0 . For CO₂ laser light at 10.6 μm , this critical density is $n_c \approx 10^{19} \text{ cm}^{-3}$ and an important part of the ICF program is an understanding of how laser light is absorbed at this surface.

Backscatter Diagnostic Facilities

In Helios, the 10 kJ eight-beam CO₂ fusion laser system in Los Alamos, the beam paths are situated such that it is relatively easy to accept a sample of the direct backscattered light from the f/2.4 focusing optics inside the target chamber. As illustrated in Fig. 1 the 16-inch-diameter NaCl output windows on the CO₂ power amplifiers are tilted at 10° to the beam paths. Since these

windows are anti-reflection coated for $10.6\text{ }\mu\text{m}$ on one side only, the uncoated side provides a 4% Fresnel reflected sample of the retropulse, which is headed directly back into the amplifier.

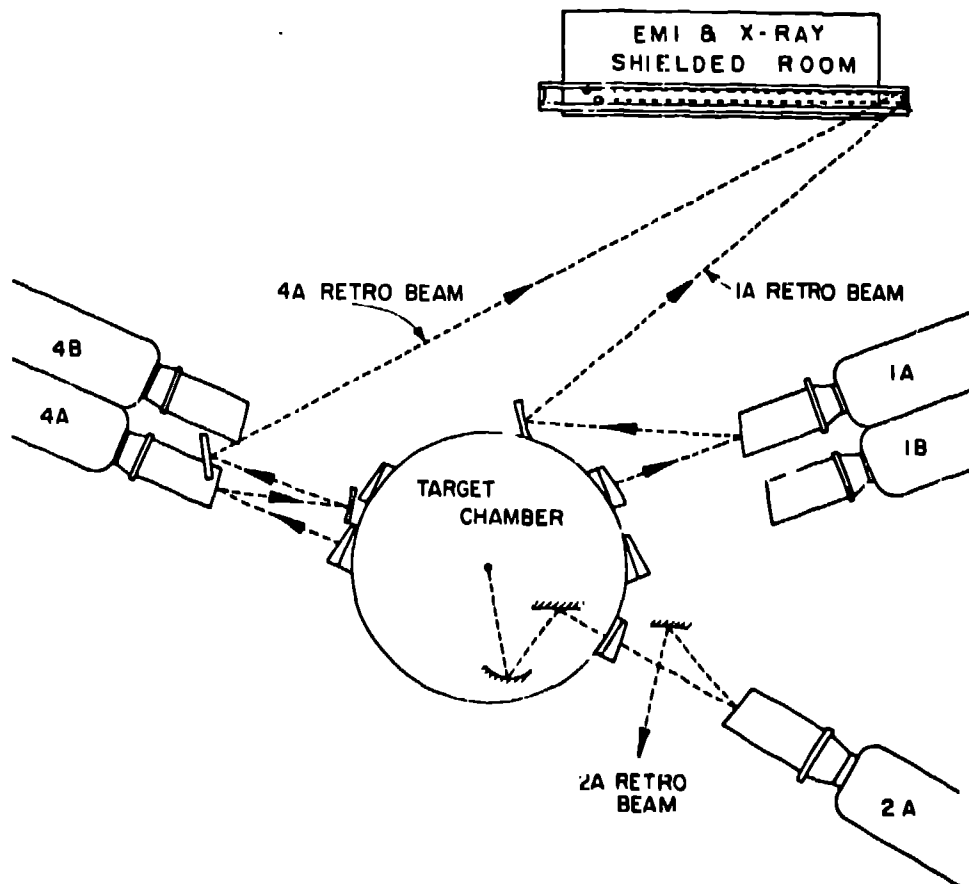


Figure 1. Optical beam paths in Helios showing three retro-channels; the 1A/4A backscattered beams focus down and pass through waveguide shields in the diagnostic screen room. The 2A backscattered beam from the $f/2.4$ off-axis paraboloid inside the target chamber (shown) is relayed to the forward-going diagnostic screen room. Amplifiers 2B, 3A, and 3B have been omitted for clarity.

Figure 1 shows that there are a total of three beamlines for which there are 16-inch-diameter focusing mirrors on the retrobeams. Lines 1A and 2A are new optical trains which focus backscattered light into a double electrically isolated and lead-lined screen room that will be devoted to backscatter diagnostics. The 2A retrochannel has been operational for a year and shares the screen room facility with the eight forward-going beam diagnostics samples; all the data presented in this paper were obtained from the 2A retro-channel.

Energy Measurements

In all cases the energy measurements in the 2A retrochannel utilized pyroelectric joulemeters whose outputs were recorded on storage oscilloscopes. Harmonic energy measurements were made with bandpass interference filters in front of the joulemeters; the ratio of harmonic energy content to total backscattered energy was obtained by placing a NaCl splitter before the harmonic filter and measuring the total spectrum. With the exception of the "double-pulse" experiment, all shots refer to a nominal 1-ns pulse width with up to 1 kJ of energy in the forward-going 2A beamline. The backscattered energy measurements are summarized in Table I which is a compilation of > 100 total shots.

TABLE 1

Target Type	Irradiation	$\frac{E_{\text{back}}}{E_{\text{forward}}}$	$\left(\frac{2\omega_0}{\omega_0}\right)_{\text{back}}$	$\left(\frac{3\omega_0}{\omega_0}\right)_{\text{back}}$	$\left(\frac{3.2\omega_0}{\omega_0}\right)_{\text{back}}$
Glass Microballoon uncoated; Cr, Au or W coated	$\sim 5 \times 10^{15} \text{ W/cm}^2$ Normal Incidence	$\frac{51\text{J}}{800\text{J}}$ (6.4%)	$\frac{0.73\text{J}}{51\text{J}}$ (1.4%)	$\frac{0.15\text{J}}{51\text{J}}$ (0.3%)	-0-
Au Shell	$\sim 5 \times 10^{15} \text{ W/cm}^2$ 53° off normal	$\frac{14.4\text{J}}{928\text{J}}$ (1.6%)	$\frac{0.14\text{J}}{14.4\text{J}}$ (1.0%)	—	—
Solid Glass	$\sim 5 \times 10^{15} \text{ W/cm}^2$ Double Pulse	$\frac{46\text{J}}{1028\text{J}}$ (4.5%)	—	—	$\frac{4\text{mJ}}{46\text{J}}$ (0.01%)

Backscattered energies from the Helios 2A retro-channel. All tabulated energies are those which would be measured at the target based on Fresnel-reflected samples of both the incident and reflected light. Harmonic energies are expressed as a fraction of the total backscattered energy.

The following conclusions can be drawn from these tabulated energies:

1. The direct backscattered energy at these high intensities ($>10^{15} \text{ W/cm}^2$) is always a small fraction ($<10\%$) of the incident energy. Although there is a lot of fluctuation in the data the average reflected energy is about 6% of the incident 2A energy.
2. The total direct backscattered energy from the 1-ns laser pulse at normal incidence on a glass microballoon (GMB) target is relatively independent of the coating material on the GMB. The data shown include shots on bare GMBs, and GMBs with CH, Cu, Au, and W coatings.
3. Most of the direct backscatter is specular; the reflected energy drops by a factor of 3 to 4 when the target normal is rotated away from the incident laser light. This was observed both with 2-mm-diameter gold shells, for which the laser light was incident at 53° to the normal and for flat Cu targets for which the laser light was 55° to the target normal.
4. Roughly 20% of the observed backscattered energy is due to scattering and/or refraction through the target plasma of energy from beamlines other than 2A. This observation is based on ~ 6 shots for which the entire system except for 2A was fired, and the 2A retrochannel recorded energy at approximately 20% of the value which would have been recorded had the 2A beamline been operating.

5. The low harmonics of the 10.6 μm laser light are created quite copiously in the target plasma, with the second harmonic alone accounting for more than 1% of the total backscatter. This is a somewhat higher yield than has been observed on flat targets at lower intensity (10^{14} W/cm^2) [1]. However, the ratio of third to second harmonic production, 1/5, is approximately the same as in Ref. [1].

Since the harmonics are generated near the surface where the incident laser light is absorbed, i.e., the critical surface, then any spectral, temporal, or spatial information obtained relates directly to the critical surface. The second harmonic spectrum, for example, may provide a convenient decoupling of the backscattered 10.6 μm spectral shifts due to stimulated Brillouin scattering and Doppler shifts from the motion of the critical surface, since the second harmonic should not be affected by Brillouin scattering.

6. The $3/2\omega_0$ harmonic has never been observed within the limits of sensitivity of the pyroelectric joulemeters, from single pulse irradiation of GMB targets at Helios. It was observed, however, on all five shots of a double-pulse experiment in which two 1-ns pulses separated by 11 ns were injected into the 2A beamline and irradiated a solid glass 300 μm diameter spherical target. This result should not be surprising, since the presence of the $3/2\omega_0$ harmonic

is indicative of a shallow density profile in the target plasma. The $3/2\omega_0$ harmonic is generated by the 2-plasmon decay instability at quarter-critical density. This instability is enhanced when there is a relatively large amount of underdense plasma near quarter critical density. This is the case when the first 1-ns pulse creates a plasma on the surface of the target, and the plasma expands freely for 11 ns. It is the interaction of the second 1-ns pulse with the underdense plasma from the first pulse which produces $3/2\omega_0$. This is a potentially useful diagnostic tool in that any temporally, spectrally or spatially resolved $3/2\omega_0$ relates directly to the quarter-critical surface.

Stimulated Brillouin Scattering

Stimulated Brillouin scattering (SBS) is a plasma instability in which an incoming photon at frequency ω_0 decays into an ion acoustic wave at frequency ω_i and a backscattered photon at ω_s following the relationship

$$\omega_0 = \omega_s + \omega_i$$

such that $\omega_i \ll \omega_s$. The signature for this process is a slightly redshifted backscatter spectrum where the amount of red shift is related to the plasma temperature at the scattering site[2]. Quantative measurements of SBS red shift, however, must unfold spectral shifts due to the Doppler effect. Recently a great deal of theoretical work on laser light induced SBS has been undertaken [3, 4], since this process represents a loss mechanism in

the coupling of laser light to the target. Experimentally it has been observed that SBS from 10.6 μm laser plasmas saturates at relatively low values [5-8] and this work is no exception. Even in the extreme case of the double-pulse experiment listed in Table 1 where SBS should have been enhanced in the underdense plasma the total backscatter was less than 5% of the incident energy, and of this only a small fraction may be a Brillouin component. Theoretical interpretations of the causes of SBS saturation include ion heating and trapping [3, 4], density profile steepening effects [9], and wave breaking [10], and in general imply a limitation on the amplitude of the ion wave that can build up in the target plasma.

Spectrally Resolved Backscatter

Backscattered spectra from the 2A retrochannel were obtained with a 3/4 m Jarrell-Ash spectrometer inside the diagnostic screen room. The detector placed at the exit focal plane of the spectrometer is a 32-element high resolution pyroelectric array* with elements on a 100 μm center to center spacing. A 50 line/mm grating produces sufficient dispersion such that successive rotational lines in the CO_2 10.6 μm P-branch [e.g. P(18) and P(20)] are separated by nine elements in the array. The overall resolution as determined by the entrance slit width and diffraction-limited spot size from the final mirror in the spectrometer is approximately 40 \AA at 10.6 μm , or one-fifth the 200 \AA separation between P(18) and P(20). With this resolution the sensitivity to motion of the critical surface via Doppler shifted backscatter is approximately 5×10^6 cm/sec. The shift in

*Manufactured by Spiricon, Inc.

wavelength $\Delta\lambda$ of light that is reflected from a moving critical surface is given by

$$\frac{\Delta\lambda}{\lambda} = 2 \frac{v_c}{c} \quad (1)$$

where λ is the wavelength of the incident light, c is the velocity of light, and v_c the velocity of the critical surface.

The response of the spectrometer to a multiline oscillator pulse from the Helios front end is shown in the lower trace of Fig. 2. This calibration was obtained by retroreflecting the weak front end pulse from an alignment sphere at the center of the target chamber. The upper trace in Fig. 2 is an actual backscattered spectrum from a 1-ns pulse on a spherical Cu target. Clearly the backscattered spectrum is substantially broadened, to the extent that there is overlap from adjacent rotational lines. Since the relative amplitudes of these lines is not routinely monitored at the output of the power amplifiers, interpretations of a red or blue shifted peak will be simplified when the oscillator is operated on a single rotational line.

With a response time of approximately 1 ms, the detector array produces a time-integrated spectrum of the 1-ns pulse. If there is both a Doppler red shift (critical surface moving radially inward) and a blue shift (critical surface moving radially outward) at different times during the pulse, the resulting spectrum is simply broadened and the usefulness of the spectrum remains in determining an approximate upper limit to the velocity of the critical surface.

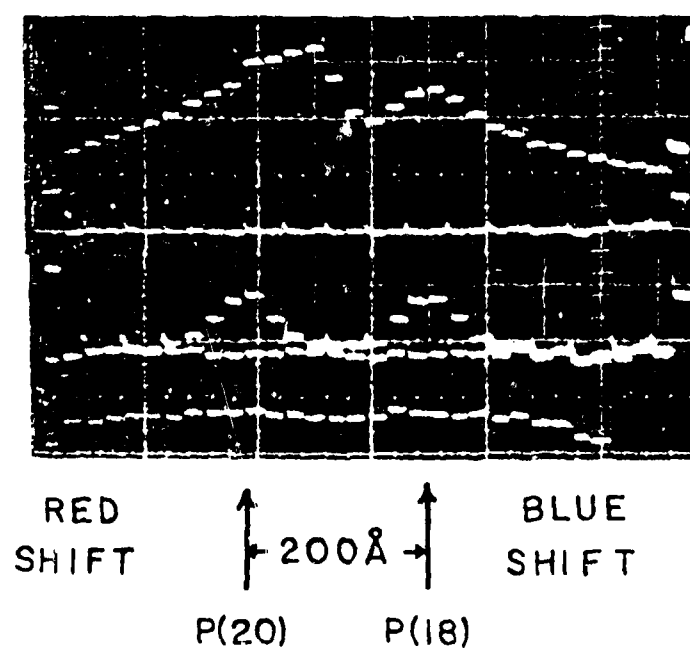


Figure 2. (a) The backscattered 10.6 μm spectrum from a Cu target using the 3/4 m spectrometer and high-resolution pyroelectric array detector. (b) The calibration trace showing the P(18) and P(20) lines from the Helios multiline front end oscillator.

This limit includes any contribution to red shift from stimulated Brillouin scattering. From the spectrum shown and from the few other spectra obtained on similar targets, no peak is shifted by more than 80 Å, and no substantial contribution to a broadened line is coming from more than 200 Å from the line center. Equation (1) then yields a conservative upper limit on the critical surface velocity at 3×10^7 cm/sec.

Temporally Resolved Backscatter

Figure 3 shows a temporally resolved 10.6 μm backscatter pulse from a 300-μm-diameter glass target. The detector used for this measurement is a modified Molelectron P5-00 fast pyroelectric and a Los Alamos 5 GHz oscilloscope. The calibration trace superimposed on the pulse shape was obtained from a 3.5 GHz signal generator. While the incident pulse (not shown) is smoothly varying in time, the backscattered pulse clearly shows some structure which may be indicative of the growth and decay of instabilities in the plasma. Temporal structure has been observed in other 10.6 μm backscatter experiments [6, 7] although no effort has apparently been made to quantitatively relate observed structure to any theoretical models.

Temporally resolved harmonics of the 10.6 μm laser light should prove to be a useful diagnostic since these are generated at the critical surface. Timing of the fundamental backscatter and of the harmonics relative to the incident pulse, something which has not yet been achieved at Helios, should yield time dependent absorption data of great interest in the theoretical simulations of the laser plasma interactions.

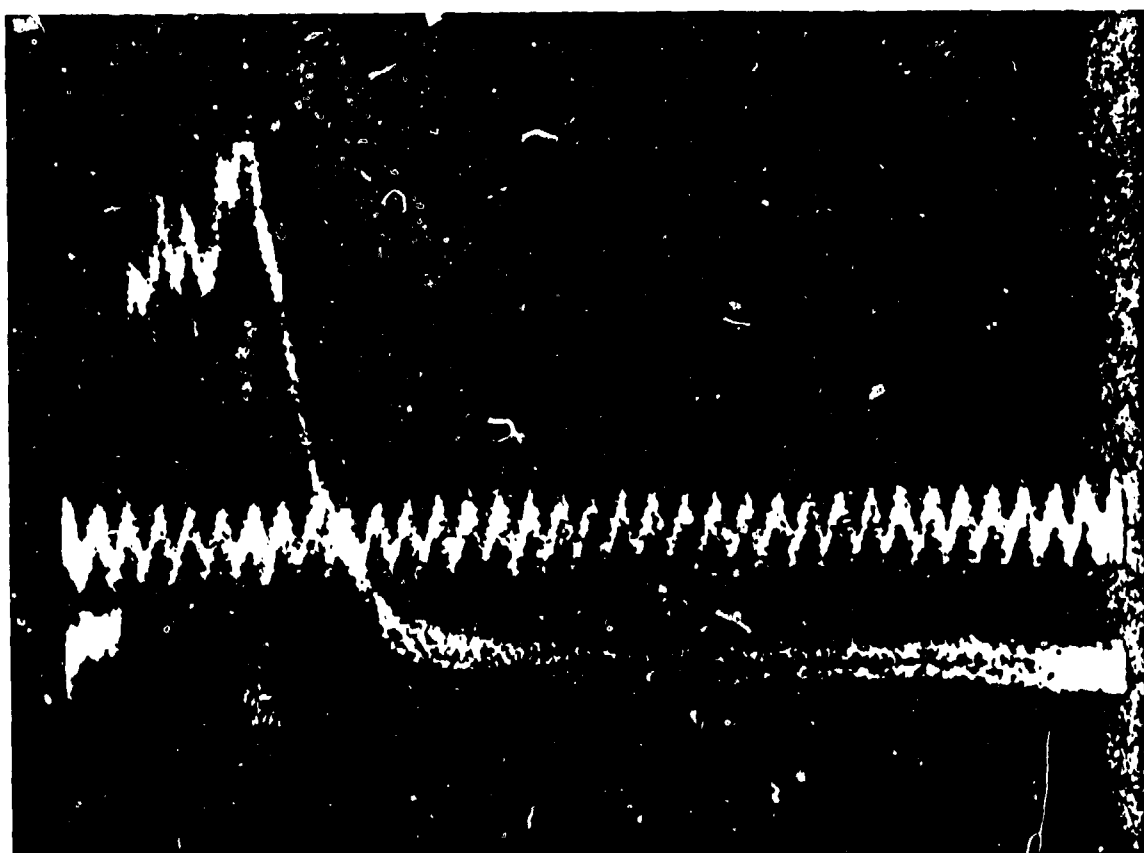


Figure 3. Temporally resolved backscatter from a solid glass target using a fast pyroelectric detector and 5 GHz oscilloscope.

Acknowledgements

I would like to thank R. Pretzel for assistance in data taking and the staff and operations crews of the Helios laser facility for providing support during the data-taking phase of the 2A retro-channel work and during the construction phase of the 1A/4A retrochannel facility.

References

- [1] N. H. Burnett, H. A. Baldis, M. C. Richardson and G. D. Enright, Appl. Phys. Lett. 31, 172 (1977).
- [2] Francis F. Chen, Report No. UCLA PPG-486, 1980 (unpublished). This is the written version of a review paper presented at the International Conference on Plasma Physics, Nagoya, Japan, on April 11, 1980.
- [3] D. W. Forslund, J. M. Kindel and E. L. Lindman, Phys. Fluids 18, 1002 (1975).
- [4] D. W. Phillicon, W. L. Kruer, and V. C. Rupert, Phys. Rev. Lett. 39, 1529 (1977).
- [5] K. B. Mitchell, T. F. Stratton and P. B. Weiss, Appl. Phys. Lett. 27, 11 (1975).
- [6] A. A. Offenberger, M. R. Cervenak, A. M. Yam, and A. W. Pasternak, J. Appl. Phys. 47, 1451 (1976).
- [7] A. Ng, L. Pitt, D. Salzmann, and A. A. Offenberger, Phys. Rev. Lett. 42, 307 (1979).
- [8] M. J. Herbst, C. E. Clayton and F. F. Chen, Phys. Rev. Lett. 43, 1591 (1979).
- [9] R. E. Turner and L. M. Goldman, Phys. Rev. Lett. 44, 400 (1980).
- [10] D. W. Forslund, J. M. Kindel, K. Lee, and B. B. Godfrey, Phys. Fluids 22, 462 (1979).